JOURNAL OF GEOPHYSICAL RESEARCH, VOL. 86, NO. B10, PAGES 9397-9410, OCTOBER 10, 1981

RADON CONTENT OF GROUNDWATER AS AN EARTHQUAKE PRECURSOR: EVALUATION OF WORLDWIDE DATA AND PHYSICAL BASIS

Egill Hauksson

Department of Geological Sciences and Lamont-Doherty Geological Observatory, Columbia University
Palisades, New York 10964

Abstract. The properties of a worldwide data set of 91 radon (^{222}Rn) anomalies (the frequency of occurrence, the precursor time interval, and the distribution of peak amplitudes) are correlated with earthquake data such as the respective magnitude and epicentral distance. These anomalies were reported as precursors to earthquakes in the United States, USSR, China, Japan, and Iceland. Although the data set is incomplete and limited by experimental deficiencies, several consistent patterns emerge. Radon anomalies from different tectonic regions show similar patterns. The radon anomalies occur at greater epicentral distances for earthquakes of the larger magnitude. Anomalies preceding large earthquakes ($M \geq 6$) are frequently observed at a distance of 100 to 500 km. These distances are larger than several times the rupture dimensions of the future earthquakes. The time from the onset of an anomaly to the time of the earthquake (the precursor time) increases with magnitude but decreases with distance between epicenter and radon station. In addition, radon anomalies are observed more frequently prior to large earthquakes than prior to small ones, indicating that the preparation zone increases in size as magnitude increases. The peak amplitude does not scale with magnitude but forms a consistent pattern with epicentral distance in that the larger the earthquake magnitude, the farther away the largest amplitudes tend to occur. The preparation zone of the earthquake where the anomalies occur forms an almost continuous annulus that expands with time away from the future rupture zone. The outer radius of this annulus scales with the earthquake magnitude. Model calculations indicate that strain fields of at most 10^{-6} to 10^{-8} strain caused the radon anomalies. If these strains are divided by the appropriate precursor time, minimum strain rates from 10^{-7} day^{-1} to 10^{-10} day^{-1} are obtained. Such small strains and strain rates suggest that in most cases neither mechanical crack growth induced by dilatancy nor mechanical coupling between pore pressure and the rock matrix caused the anomalies. Large changes in the orientation of the local strain field, however, could occur and affect the local stress intensity factor. Since changes in the stress intensity factor can result in stress corrosion, the occurrence of radon anomalies is attributed to slow crack growth controlled by stress corrosion in a rock matrix saturated by groundwater.

Introduction

Variations in radon (^{222}Rn) content of groundwater that have been observed prior to some earthquakes constitute an important nonseismic precursor to earthquakes. Active national programs for radon monitoring in the United States, USSR, People's Republic of China, Japan, and Iceland have reported at least 91 anomalies associated with some 46 different earthquakes during the last 15 years. The basic features of the radon precursor are poorly understood, and currently, only Chinese scientists actually use local radon data in conjunction with other precursory data as a basis for issuing earthquake predictions.

To establish the properties of changes in radon content as an earthquake precursor, this paper evaluates the main features of the worldwide data set of radon anomalies and proposes growth of small tensile cracks, controlled by stress corrosion, as a physical basis for the anomalies. Since there is considerable scatter in the data set, only qualitative analysis and interpretation of the main features are attempted. The main features of the radon data set (the frequency of occurrence, the precursor time interval, and the distribution of peak amplitudes) are correlated with earthquake data such as the respective magnitude and epicentral distance.

It is likely that the results of the analysis will be influenced by experimental deficiencies. Such deficiencies could consist of not looking for anomalies prior to small earthquakes, large spacing between radon stations compared with the rupture dimensions of small earthquakes, and infrequent sampling. Nonetheless, a closer analysis of the data is warranted if it can aid in identifying possible consistent patterns in this data set.

This paper does not address such features as false alarm rate or nonoccurrence of radon anomalies because those data are generally not available in the literature. A comparison of the properties of radon anomalies with the properties of other precursors is also not considered.

Previous syntheses of radon anomalies and other types of earthquake precursors were all based on a much smaller data set than is treated here. Scholz et al. [1973] interpreted two radon anomalies and numerous other precursors in terms of the dilatancy diffusion model. They found a log-linear relationship between the precursor time and the earthquake magnitude. Rikitake [1975, 1979] used worldwide data to correlate the precursor time interval and earthquake magnitude. He found that a systematic correlation between precursor time and magnitude is more often the exception than the rule for earthquake precursors. A summary of recent radon data from the People's Republic of China is presented by Wakita [1978] and Teng [1980b]. Teng [1980b] emphasizes the importance of

Paper number 1B1247.
0148-0227/81/001B-1247$01.00

short-term spikelike anomalies preceding the impending earthquake by days. Asimov et al. [1979] review recent results from Soviet Central Asia and point out that the radon precursor showed promising results in terms of estimating the size and the time but not the location of a future earthquake.

Initially, the dilatancy diffusion model and several other similar models suggested that the radon anomalies were related to mechanical crack growth in the volume of dilatancy or to changes in flow rate of groundwater [Ulomov and Mavashev, 1971; Scholz et al., 1973]. The drawback with this explanation is that it often requires an unreasonably large volume of dilatant material and very large changes in stress or strain far away from the subsequent epicenter. In a review paper on stress corrosion theory, Anderson and Grew [1977] first proposed an alternative mechanism. It attributes the radon anomalies to slow crack growth controlled by stress corrosion in a rock matrix saturated by groundwater. They argue that crack growth by stress corrosion should precede any mechanical cracking in a wet environment. Subsequently, Atkinson [1979, 1980] and Wilkins [1980] confirmed experimentally that geologic materials can suffer crack growth at very low strain rates in the presence of high humidity. The mechanism of stress corrosion suggests that the occurrence of radon anomalies may depend on strain rate and local conditions such as rock type, elastic moduli, pattern of microcracks, degree of saturation, temperature, stress intensity factor, and hydraulic properties.

Description of Radon Data

The groundwater radon data reported in the literature consist of some 91 anomalies that have been related to 46 different earthquakes. Several large earthquakes of magnitude greater than 6.5 have been preceded by up to 10 different anomalies. Most small earthquakes, however, have been preceded by only one anomaly.

Tables 1 to 6 list earthquakes for which one or more radon anomalies have been reported. The epicentral locations were confirmed by using the International Seismological Center or the Preliminary Determination of Epicenters bulletins. In most cases the associated radon anomalies were originally presented by the investigators who are referred to in the tables. The investigators commonly display the data as a time series to illustrate shape, precursor time interval, and amplitude of an anomaly. These parameters were defined (either by the original investigator or in this paper) as described below and given numerical values that are listed in Tables 1 to 6.

The relative peak amplitude of each anomaly is the highest value of radon emission observed during the anomaly, divided by the background radon content observed prior to the onset of an anomaly. This method of amplitude determination does not take into account the sampling interval of the radon data. If rapid fluctuations of large amplitude (as, for example, observed by Shapiro et al. [1981]) are present, the value of the relative amplitude is overestimated. If the data, on the other hand, were time averaged before publication (such as most of the Chinese data), the value of the relative amplitude is underestimated. In the cases where samples are collected infrequently, such as biweekly or monthly, the method probably gives a fair estimate of the amplitude as long as the precursor time is of the order of several times the sampling interval of the radon data. Although the method for determining relative amplitudes is plagued by these deficiencies, it permits simple and rapid evaluation of relative amplitudes and clearly reflects the observed range of amplitudes of radon anomalies.

The time of onset of the precursor time interval is the time when the trend of the data changes suddenly because an increase or decrease in radon emission occurred. The end of the precursor time interval is taken to be the time of the earthquake, since in most of the cases the radon emission returned to normal levels approximately at that time. A quality factor ranging from A to D was also assigned to each anomaly. If both the beginning and the end of an anomaly are easily identified, it is assigned a quality of A. If either of these is unclear, it is assigned a quality of B. If both are unclear, a quality of C is assigned. If an anomaly could be coseismic or a precursor to more than one earthquake or if its amplitude is less than the normal background fluctuations, it is given a quality of D and is not included in the analysis of the data. In addition, the distance between epicenter and radon station and the name and type of the station (e.g., well (W) or spring (S)) are tabulated.

The uncertainties that are associated with each datum in Tables 1 to 6 are not tabulated or included in the figures for several reasons. First, the original investigators rarely included any uncertainties or basic data that would permit quantitative estimates of the uncertainty. Second, in most cases, experimental errors are much smaller than errors that arise from the subjective estimates of the parameters of the anomaly such as the precursor time interval. If a sufficiently large data set is available, however, errors in the subjective estimates are reflected by the general scatter of the data points more clearly than by estimated error bars of doubtful validity. As a general guideline, however, it is noted that earthquake magnitudes can easily vary by half a magnitude unit, whereas the precursor time interval, epicentral distance, and relative peak amplitude can in most cases be determined with an uncertainty of less than 5%.

United States. The majority of the radon anomalies in Table 1 were reported by investigators working in southern California. Shapiro et al. [1980] presented 20 months of continuous radon data from the Kresge site in Pasadena. They found that three out of a set of 11 small earthquakes that occurred in 1977 and 1978 were preceded by a change in radon emission. On the basis of weekly samples of 14 wells in southern California, Teng [1980a, b] described possible radon anomalies that preceded the Big Bear (1979), Malibu (1979), and Pearblossom (1976) earthquakes. During the summer of 1979, several cases of anomalous radon emissions were reported [Craig et al., 1980; Shapiro et al., 1981]. On

the basis of geodetic data, Savage et al. [1981] suggest that a large-scale, dynamic strain event occurred in the Transverse Ranges in 1979 and early 1980. Shapiro et al. [1981] discussed the possibility that the strain event triggered the onset of radon anomalies and the Imperial Valley (1979), Malibu (1979), and Lytle Creek (1979) earthquakes. Craig et al. [1980], who collected samples at monthly intervals, explained their observations of anomalous radon emission, as well as other gases, as a possible precursor to the nearby Big Bear (1979) earthquake. In Table 1 the data from Craig et al. are included as a precursor to both the Big Bear and the Imperial Valley earthquakes, since the anomalous radon emission continued until the time of the Imperial Valley earthquake.

In addition, several studies of radon emission in surface soil using alpha track film cups have been carried out (see, for example, King [1980]). These data are not included here, since radon emission in surface soil is more susceptible to meteorological disturbances than radon content of groundwater. Furthermore, it has not been established that these two types of data are compatible.

USSR. The pioneering work of investigating changes in radon content preceding local earthquakes was carried out by scientists in the USSR approximately 15 years ago. Table 2 contains data from the initial studies in Tashkent by Ulomov and Mavashev [1971] and Antsilevich [1971]. These studies included the 1966 Tashkent earthquake of magnitude 5.3 and several single shocks in the magnitude range from 3.0 to 4.0 that occurred in the same area in 1967. The wells used for radon sampling were situated on top of the seismic activity that clustered within the city of Tashkent at a depth interval of 0 to 7 km. In Table 2 the epicentral distance in all these cases is assumed to be 5 km, since the exact locations of the wells and the earthquake are unavailable. Most of the anomalies have an easily identifiable precursor time and peak amplitude except for the very first reported radon anomaly, which has an unclear onset caused by a gap in the data from 1961 to 1965.

Asimov et al. [1979] reviewed recent radon data from Soviet Central Asia. They correlated change in radon content observed in the Tashkent, Andizhan, Dushanbe, and Alma-Ata areas with the regional seismicity. They presented a map of each area that showed several radon stations in a cluster. Unfortunately, the locations of the radon data that are shown in different figures in their paper are given only by general area, not by name of the station within an area. This introduced some uncertainty into the epicentral distance estimates in Table 2. Since Asimov et al. rarely gave time duration or peak amplitude, these were determined in this paper from the data shown in their figures. The most outstanding anomalies were observed prior to the Markansu (1974), Gazli (1976), and Alma-Ata (1978) earthquakes. The other anomalies are less distinctive, since the observed variations are more gradual and of lower amplitude and thus somewhat smeared out by background noise.

People's Republic of China. Radon data from northeast China, the provinces of Hopeh and Liaoning and the city of Peking, that are presented in Table 3 include anomalies associated with three large earthquakes, Pohai Bay (1969), Haicheng (1975), and Tangshan (1976).

The Haicheng earthquake (1975) of magnitude 7.3 was predicted partly on the basis of radon anomalies that were later reported by Raleigh et al. [1977] and Teng [1980b]. At two stations, Tanggangzi and Shenyang, both long- and short-term anomalies can be identified in the data. An anomaly at Liaoyang that showed increasing radon emission several hours before the earthquake and peaked a day later is considered to be coseismic here. The anomaly at Panshan was given a quality of D, since it was possibly contaminated by seasonal changes related to local rainfall [Raleigh et al., 1977].

The Tangshan earthquake (1976) was not predicted, but in retrospect several precursors including anomalous radon emissions were identified [Wang, 1978; Wakita, 1978; Jiang and Deng, 1980]. Except for two rather unclear short-term anomalies, the radon data are characterized by small amplitudes and a lack of distinctive increase in activity as the time of the earthquake approached. Two very long term anomalies were reported at the stations Kuanchuang and Ankochuang, lasting for 970 days and 1370 days, respectively. The stations Tientsin and Luanxian, which were assigned a quality of D, showed rapid fluctuations during the early spring of 1976 and normal emission of radon for several weeks preceding the earthquake.

Table 4 contains eight short-term anomalies that were observed at the same radon station, Kutzan, and numerous radon anomalies that preceded the Lungling-Lushi (1976) doublet and Songpan-Pingwu (1976) triplet of large earthquakes. The Lungling-Lushi earthquakes of magnitude 7.5 and 7.6, which occurred 1.5 hours apart, were preceded by long-term anomalies at the stations Lungling, Hsiakuan, and Iliang. Several intermediate-term anomalies and one short-term anomaly were also reported [Tang, 1978; Wakita, 1978]. It is worth noting that most of the anomalies had very low amplitudes (less than 30%) and the available data go back at least 4 years. The Songpan-Pingwu earthquakes of magnitude 7.2, 6.7, and 7.2 were preceded by several long- and short-term radon anomalies [Wallace and Teng, 1980]. Five out of 10 anomalies had a negative amplitude, which is an unusually high ratio, and two stations showed both long- and short-term anomalies. The properties of the radon anomalies associated with the Lungling-Lushi and Songpan-Pingwu earthquakes appear to scale with distance between the epicenter and the respective radon station [Tang, 1978; Szechwan Provincial Seismology Bureau (SPSB), 1979].

Japan. Wakita et al. [1980a] presented a radon anomaly that preceded the Izu-Oshima-Kinkai earthquake (1978) of magnitude 7.0. The data were collected using a continuous radon monitoring meter and revealed a complicated pattern of anomalous radon emission. In Table 5, both long- and short-term anomalies are listed.

Iceland. Hauksson and Goddard [1981] reported nine radon anomalies that preceded several different earthquakes in the magnitude

TABLE 1. U.S. Earthquakes and Precursory Radon Anomalies

Date	Magnitude	State	Location	Latitude	Longitude	Radon Station	Type	Amplitude Relative	Duration, days	Quality	Epicentral Distance, km	Reference
Nov. 22, 1976	3.5	California	Pearblossom	34.523N	117.965W	SC	S	36%	31	C	25	Teng [1980b]
Feb. 23, 1977	2.3	S. Carolina	Jocasse	34.953N	82.940W	LJ	S	-50%	14	C	1	Talwani et al. [1980]
Sep. 24, 1977	2.9	California	Pasadena	33.960N	117.833W	KPAS	W	62%	3	A	21	Shapiro et al. [1980]
Dec. 20, 1977	2.8	California	Pasadena	33.953N	118.170W	KPAS	W	25%	9	A	12	Shapiro et al. [1980]
Jan. 01, 1979	4.7	California	Malibu	33.950N	118.683W	KPAS	W	72%	42	B	54	Shapiro et al. [1980]
						SHS	S	225%	82	A	20	Teng [1980a]
June 28, 1979	5.0	California	Big Bear	34.250N	116.900W	BP	W	310%	12	B	85	Teng [1980a]
						AROW	S	72%	45	A	31	Craig et al. [1980]
Oct. 15, 1979	6.6	California	Imperial Valley	32.633N	115.333W	KPAS	W	400%	116	B	335	Shapiro et al. [1981]
						DAT	W	200%	95	B	310	Shapiro et al. [1981]
						AROW	S	72%	145	B	265	Craig et al. [1980]
						LYCR	W	64%	2	B	260	Shapiro et al. [1981]

TABLE 2. USSR Earthquakes and Precursory Radon Anomalies

Date	Magnitude	Location	Latitude	Longitude	Radon Station	Type	Amplitude Relative	Duration, days	Quality	Epicentral Distance, km	Remarks	Reference
Apr. 26, 1966	5.3	Tashkent	41.3 N	69.3 E	Tashkent	W	20%	400	B	5	1	Ulomov and Mavashev [1971]
Mar. 24, 1967	4	Tashkent	41.3 N	69.3 E	Tashkent	W	100%	11	A	5	1	Ulomov and Mavashev [1971]
June 20, 1967	3.5	Tashkent	41.3 N	69.3 E	Tashkent	W	23%	3	A	5	1	Antsilevich [1971]
July 22, 1967	3.5	Tashkent	41.3 N	69.3 E	Tashkent	W	20%	3	A	5	1	Antsilevich [1971]
Nov. 09, 1967	3.0	Tashkent	41.3 N	69.3 E	Tashkent	W	23%	8	A	5	1	Antsilevich [1971]
Nov. 17, 1967	3.3	Tashkent	41.3 N	69.3 E	Tashkent	W	23%	7	A	5	1	Antsilevich [1971]
Dec. 17, 1967	3.0	Tashkent	41.3 N	69.3 E	Tashkent	W	23%	4	A	5	1	Antsilevich [1971]
1969		Fergana	40.4 N	71.3 E	Tashkent	W	23%	13	D		2	Rikitake [1975]
Feb. 13, 1973	4.7	Uzbekistan			Obi-Garm	W	47?	5	A	130		Mirzoev et al. [1976]
Aug. 11, 1974	7.3	Markansu	39.39N	73.9 E	Alma-Ata	W	100%	100	B	530	1	Asimov et al. [1979]
Feb. 12, 1975	5.3	Tien Shan	43.16N	78.97E	Alma-Ata	W	10%	110	C	100	1	Asimov et al. [1979]
May 17, 1976	7.3	Gazli	40.35N	63.45E	Tashkent	W	220%	4	A	470		Sultanxodjoev et al. [1976]
					Obi-Garm	W	25%	90	C	550		Asimov et al. [1979]
Jan. 31, 1977	6.6	Isfarin-Batnen	40.04N	70.85E	Tashkent	W	-30%	60	C	190		Asimov et al. [1979]
					H-O-Garm	W	-20%	125	C	200		Asimov et al. [1979]
Mar. 24, 1978	7.1	Alma-Ata	42.84N	78.61E	Alma-Ata	W	32%	50	A	65		Asimov et al. [1979]
Nov. 01, 1978	6.7	Zaalai	39.42N	72.71E	Obi-Garm	W	-30%	470	B	270		Asimov et al. [1979]
					Yavros	W	-40%	470	B	300		Asimov et al. [1979]
					Andizhan	W	20%	75	C	150		Asimov et al. [1979]
					Andizhan	S	-20%	70	C	150		Asimov et al. [1979]

Remarks are (1) exact radon station location not well known, and (2) not plotted or included in analysis, listed for completeness.

TABLE 3. People's Republic of China: Hopeh and Liaoning Provinces Earthquakes and Precursory Radon Anomalies

Date	Magnitude	Province	Location	Latitude	Longitude	Radon Station	Type	Amplitude Relative	Duration, days	Quality	Epicentral Distance, km	Remarks	Reference
July 18, 1969	7.4		Pohai Bay	38.43N	119.47E	Tangku	W	60%	170	B	170		Liu et al. [1975]
						Laohsi	W	40%	190	C		1	Liu et al. [1975]
						Yachang	W	70%	190	C		1	Liu et al. [1975]
						Paoti	W	60%	190	C	230		Liu et al. [1975]
Aug. 05, 1971	4.3	Hopeh	Ningshin	37.6 N	114.9 E	Shankou	W	200%	40	B	42		Liu et al. [1975]
June 06, 1974	4.9	Hopeh	Hsingtang	37.54N	115.10E	Hownsun	W	290%	16	B	18	1	Liu et al. [1975]
						Jinti	W	-20%	19	C		1	Liu et al. [1975]
Feb. 04, 1975	7.3	Liaoning	Haicheng	40.66N	122.63E	Tanggangzi	S	38%	270	C	50		Raleigh et al. [1977]
						Tanggangzi	S	17%	50	B	50		Raleigh et al. [1977]
						Panshan	Wl	10%	150	D	90	2	Raleigh et al. [1977]
						Liaoyang	S	100%	1	D	85	2	Teng [1980b]
						Shenyang	W	-43%	66	A	140		Raleigh et al. [1977]
						Shenyang	W	20%	8	C	140		Raleigh et al. [1977]
July 27, 1976	7.8	Hopeh	Tangshan	39.56N	117.87E	Tangshan		30%	5	D	5	2	Wang [1978]
						Ankochuang		15%	970	B	50		Wakita [1978]
						Tientsin		10%	110	D	75	2	Wang [1978]
						Luanxian		5%	370	D	80	2	Wang [1978]
						Antze		50%	15	B	100		Wang [1978]
						Kuanchuang		40%	1370	B	130		Jiang and Deng [1980]
						Kuanchuang		27%	162	B	130		Jiang and Deng [1980]
Mar. 07, 1977	6.0	Hopeh	Chienan	40.10N	118.74E	Peking	W	70%	3	A	200		Teng [1980b]
May 12, 1977	6.7	Hopeh	Lutai	39.27N	117.71E	Tungchow	W	30%	1	D	115	2	Teng [1980b]

Remarks are (1) exact radon station location not well known, and (2) not plotted or included in analysis, listed for completeness.

TABLE 4. People's Republic of China: Szechwan and Yunnan Provinces Earthquakes and Precursory Radon Anomalies

Date	Magnitude	Province	Location	Latitude	Longitude	Radon Station	Type	Amplitude Relative	Duration, days	Quality	Epicentral Distance, km	Remarks	Reference
Apr. 08, 1972	5.2	Szechwan	Sahteh	29.52N	101.84E	Kutzan	S	55%	12		70	1	Teng [1980b]
Sep. 27, 1972	5.8	Szechwan	Takung	30.31N	101.63E	Kutzan	S	34%	12		54	1	Teng [1980b]
Feb. 06, 1973	7.9	Szechwan	Luhuo	31.33N	100.49E	Kutzan	S	120%	9	A	200		Wakita [1978]
Feb. 16, 1973	5.3	Szechwan	Luhuo	31.73N	100.04E	Kutzan	S	36%	2	D	260	1,2	Teng [1980b]
Apr. 22, 1973	5.2	Yunnan	Yiliang	27.61N	104.10E	Kutzan	S	41%	14		340	1	Teng [1980b]
May 08, 1973	5.2	Szechwan	Songpan	32.90N	104.03E	Kutzan	S	40%	14		345	1	Teng [1980b]
June 29, 1973	5.5	Szechwan	Mapien	28.84N	103.67E	Kutzan	S	89%	9	A	200		Wakita [1978]
May 29, 1976	7.5	Yunnan	Lungling	24.51N	98.95E	Balazhang	S		(150)	D	10	2	Wakita [1978]
						Lungling		20%	510	B	20		Wakita [1978]
						Tengchung	S	8%	75	D	60	1	Tang [1978]
						Hsiakuan	S	15%	425	B	190		Wakita [1978]
						Erhyuan	S	8%	160	B	210		Wakita [1978]
						Lantsang	S	12%	130	B	215		Wakita [1978]
						Yushi	S	7%	75		360	1	Wakita [1978]
						Iliang	S	20%	290	C	420		Tang [1978]
						Hsuntien	S	200%	12		450	1	Wakita [1978]
Aug. 16, 1976	7.2	Szechwan	Songpan-Pingwu	32.78N	104.09E	Songpan	S	29%	480	C	40		Wakita [1978]
						Maowen	S	11%	420	C	100		Wakita [1978]
						Wutu		20%	190	A	100		SPSB [1979]
						Kutzan	S	70%	7	A	320		Teng [1980b]
						Kutzan	S	-12%	200	C	320		Wakita [1978]
						Kangting	S	90%	48	B	340		Wakita [1978]
						Kangting	S	-60%	160	B	340		Wakita [1978]
						Tzekung		55%	160	A	390		SPSB [1979]
						Kantse		5%	108	D	410	2	SPSB [1979]
						Batang	S	110%	34	B	560		Wakita [1978]

Remarks are (1) plotted data not available, and (2) not plotted or included in analysis, listed for completeness.

TABLE 5. Japan Earthquakes and Precursory Radon Anomalies

Date	Magnitude	Location	Latitude	Longitude	Radon Station	Type	Amplitude Relative	Duration, days	Quality	Epicentral Distance, km	Reference
Jan. 14, 1978	6.8	Izu-Oshima	34.77N	139.20E	SKE-1	W	7%	230	B	25	Wakita et al. [1980a]
					SKE-1	W	-8%	7	B	25	Wakita et al. [1980a]

TABLE 6. Iceland Earthquakes and Precursory Radon Anomalies

Date	Magnitude	Location	Latitude	Longitude	Radon Station	Type	Amplitude Relative	Duration, days	Quality	Epicentral Distance, km	Remarks	Reference
July 03, 1978	2.7	SISZ	64.00N	20.35W	FL	W	380%	22	A	14	1	Hauksson and Goddard [1981]
Aug. 28, 1978	3.4	SISZ	63.94N	20.32W	LA	W	60%	17	B	5		Hauksson and Goddard [1981]
					FL	W	280%	17	A	21		Hauksson and Goddard [1981]
Oct. 30, 1978	3.8	SISZ	63.96N	20.31W	OR	W	40%	24	B	20		Hauksson and Goddard [1981]
Nov. 19, 1978	4.3	SISZ	63.99N	20.46W	FL	W	-80%	18	B	16		Hauksson and Goddard [1981]
June 29, 1979	1.9	SISZ	63.95N	20.41W	HL	W	40%	19	B	9		Hauksson and Goddard [1981]
Sep. 05, 1979	2.8	SISZ	63.97N	20.41W	HL	W	40%	17	A	8		Hauksson and Goddard [1981]
					KA	W	100%	33	A	5		Hauksson and Goddard [1981]
Dec. 15, 1979	4.1	TFZ	66.24N	16.69W	HA	W	100%	37	A	60	2	Hauksson and Goddard [1981]

Remarks are (1) Southern Iceland Seismic Zone, and (2) Tjörnes Fracture Zone.

range from 2.0 to 4.3 (see Table 6). They operated a network of seven radon stations spaced 10 to 15 km apart in a rather small area. Their results indicated that the probability of observing radon anomalies in Iceland before small earthquakes of magnitude larger than 2.0 was approximately 65%.

Evaluation of Radon and Earthquake Data

To understand the mechanism of radon anomalies and to establish earthquake prediction capability and reliability, empirical scaling relationships between the radon and the earthquake data are needed. This preliminary evaluation of the worldwide data set is intended as a first step toward this goal.

The available data set consists of properties of the radon anomalies and parameters of the associated earthquakes and is listed in Tables 1 to 6. Although this data set is larger than most comparable data sets for other earthquake precursors, it is incomplete and possibly biased by contaminated data. The data set will become more complete and more representative as more networks for radon monitoring are established and the period of observation becomes longer. Unfortunately, it is not possible to eliminate contaminated data, such as misrepresentation of noisy data as an anomaly or assigning an anomaly to an unrelated earthquake, since the original investigators who collected the data did not include all relevant seismicity and rarely accounted for possible noise in the radon data. Since these deficiencies of the data set are likely to influence the analysis of the data, this analysis is only intended to give a qualitative evaluation of the possible existence of scaling relationships. An important part of such an evaluation is to look for consistency within the data set as a whole by, for example, comparing data from different geographic regions. Furthermore, the evaluation can contribute to substantiating or refuting previously suggested scaling relationships and can help to evaluate whether the currently used research strategy is producing useful data.

Frequency of occurrence. The histogram shown in Figure 1a reveals that approximately the same number of small and large earthquakes have been reported to be preceded by at least one radon anomaly. The relationship between earthquake magnitude and the probability of a radon anomaly being observed is illustrated in Figure 1b. The stepped curve represents the cumulative number of earthquakes that were preceded by anomalies. The sloping line constitutes the Gutenberg-Richter magnitude-frequency relationship for earthquakes assuming a b value of 1.0 and a single earthquake of magnitude 8.0 [Richter, 1958, p. 361]. The Gutenberg-Richter relationship indicates that for a global average, small earthquakes are more abundant than large ones. The stepped curve and the straight line in Figure 1b show increasing divergence with decreasing earthquake magnitude. Therefore the data suggest that the probability of detecting a radon anomaly before a large earthquake is relatively much greater than detecting an anomaly before a small earthquake. This observation is more likely to be the result of the experimental

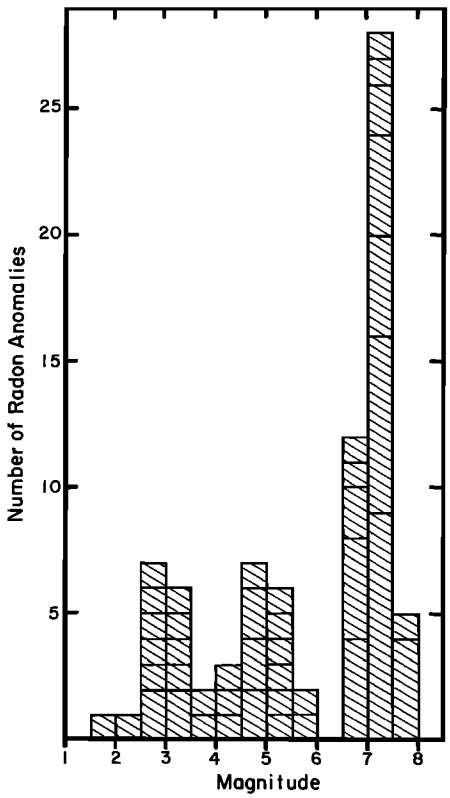

Fig. 1a. Histogram of number of radon anomalies as a function of earthquake magnitude. Anomalies that belong to the same earthquake are enclosed by a rectangle.

techniques that are applied than to be of basic geophysical significance. The set of earthquakes that usually is considered for possible correlation with a radon anomaly in most cases does not include, for example, foreshocks, aftershocks, or all earthquakes in an earthquake swarm. These events constitute a significant fraction of the average global seismicity, which is the basis of the Gutenberg-Richter relationship.

Large earthquakes appear to be preferentially preceded by more than one radon anomaly (Figure 1a). Although it is possible that this observation is caused by experimental deficiencies such as low density of radon stations, several detailed studies by Talwani et al. [1980], Shapiro et al. [1980], and Hauksson and Goddard [1981] indicate that small earthquakes are rarely preceded by more than one radon anomaly. It is worth noting that only two radon anomalies have been reported for earthquakes in the magnitude range from 5.5 to 6.5 (Figure 1a). As more data accumulate, this data gap will probably disappear.

Precursor time interval. The temporal behavior of radon anomalies and other earthquake precursors is usually treated in terms of a precursor time interval, defined as the time period from the onset of anomalous activity until the time of the earthquake. In Figure 2 the precursor time intervals of all the radon anomalies listed in Tables 1 to 6 are plotted as a function of the earthquake magnitude. The scatter of the data points indicates that an almost continuous distribution ranging from long- to short-term radon anomalies exists. The distribution appears to be independent of geographic region, since all the data sets show a similar overlapping pattern. This almost continuous distribution of precursor times can be attributed either to different intensities of preseismic deformation or to some variable, for example, epicentral distance, that could influence the precursor time. The upper boundary of the distribution reflects increasing precursor time length as the earthquake magnitude increases, which is in agreement with most theoretical models of precursor processes [Rice and Rudnicki, 1979]. The upper boundary, however, can also be influenced by a reluctance to identify long-term anomalies, which would severely violate a typical precursor time-magnitude relationship [Scholz et al., 1973; Rikitake, 1975], as precursors to small earthquakes. The lower boundary is affected by the response time of the mechanism of radon release, by local hydraulics, and by artifacts such as sampling frequency, density of radon stations, and possible environmental noise superimposed on the radon signal.

Radon anomalies frequently are reported to have occurred far away from the respective earthquake epicenters. Figure 3 shows the precursor time interval as a function of the distance between a radon station and an epicenter.

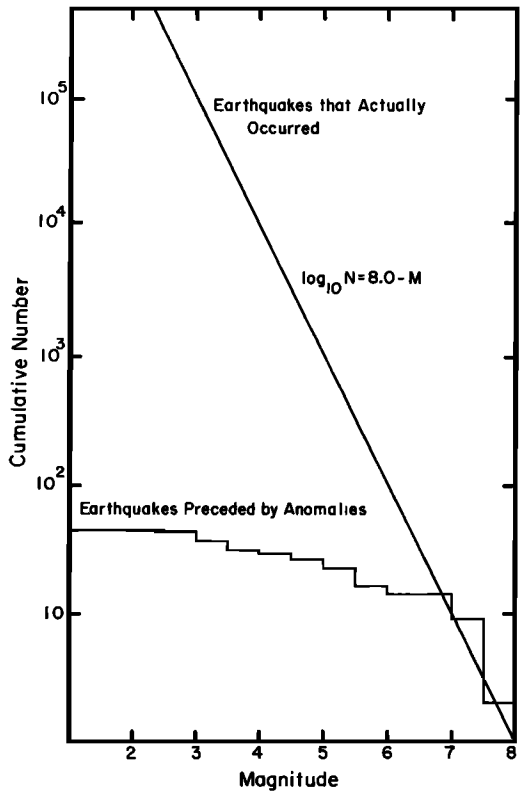

Fig. 1b. Relationship between earthquake magnitude and the probability of a radon anomaly being observed. The stepped curve represents the cumulative number of earthquakes that were preceded by anomalies. The sloping line is the Gutenberg-Richter magnitude-frequency relation.

An overall trend of decreasing precursor time with distance can be seen by dividing the data set into three different magnitude ranges, from 2 to 4, 4 to 6, and 6 to 8, which are shown unmarked, dotted, and solid, respectively, in Figure 3.

The precursor times of the small earthquakes in the magnitude range from 2 to 4 do not show a significant correlation with distance. This is probably a result of the lack of information about the exact location of some of the earthquakes, such as the Tashkent events. In addition, the unknown depth of the earthquakes probably influences the results. The precursor times of the earthquakes in the intermediate range from 4 to 6 correlate well with an inverse distance squared dependence. The precursor times of the large earthquakes, however, do not show such a strong distance dependence. The precursor time-distance dependence for the large earthquakes also is somewhat obscured by the occurrence of both long- and short-term radon anomalies at the same station. Unless long- and short-term anomalies can be distinguished, the implied distance dependence in Figure 3 cannot easily be quantified.

Thus the almost continuous distribution of precursor time interval as a function of earthquake magnitude in Figure 2 can be attributed in part to a dependence on epicentral distance. The effects of other parameters such as intensity of preseismic deformation or earthquake depth and focal mechanism are probably also of importance for explaining the observed distribution.

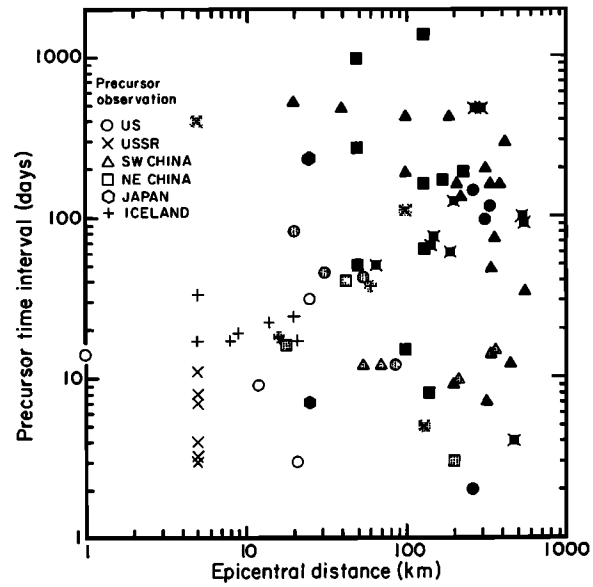

Fig. 3. Precursor time interval as a function of epicentral distance. Unmarked, dotted, and solid data points represent magnitude ranges of 2-4, 4-6, and 6-8, respectively.

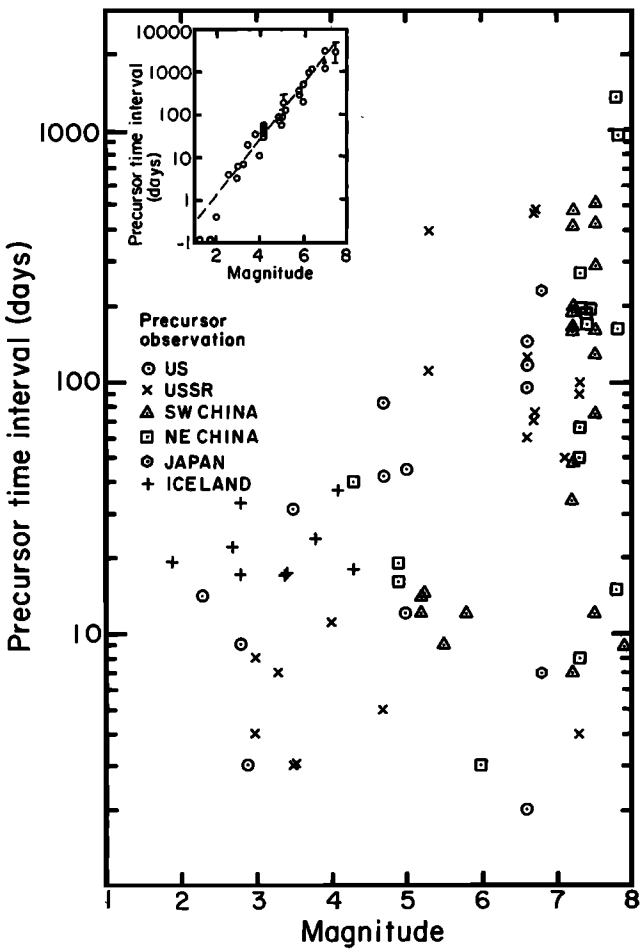

Fig. 2. Precursor time interval as a function of respective earthquake magnitude for worldwide radon data. In the upper left-hand corner is same plot from Scholz et al. [1973].

Amplitude distribution. Large amplitude anomalies are not more commonly observed at stations where the background radon content is high than at stations with low radon content. Since radon anomalies are usually considered to be generated locally (within 1 km of the respective station), the distribution of their relative amplitude could be useful for defining the spatial extent and shape of the zone of precursor deformation. Figure 4 shows the absolute value of the relative peak amplitude of the radon anomalies as a function of epicentral distance. The curves shown in the plots represent envelopes that emphasize the distances at which the largest anomalies were observed. For example, earthquakes of magnitudes between 6.0 and 8.0 have amplitudes that peak at distances of 200 to 500 km. Because future observations may reveal anomalies at even greater distances than have been reported so far, the envelopes are shown as dashed lines at large distances. In addition, clustering of large earthquakes in time, as observed in China in 1976, may cause overlapping patterns of radon anomalies, which in turn can lead to arbitrary boundaries between the zones of precursory deformation.

The size of the amplitude of a radon anomaly is probably strongly influenced by local conditions such as rock type and local hydraulics. However, it is interesting to note some of the features in Figure 4. The zone of precursory deformation appears to be rather broad, possibly a circular annulus, since almost no anomalies are observed close to the subsequent epicenter.

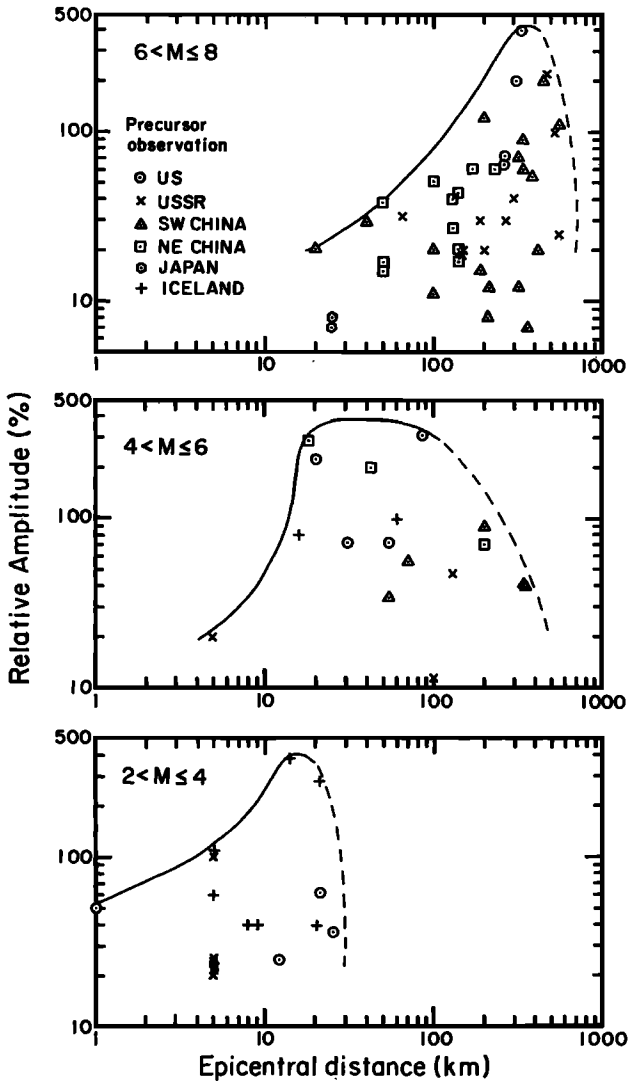

Fig. 4. Absolute value of relative amplitude as a function of epicentral distance. The envelopes emphasize at what distances the peak amplitudes tend to occur.

The lack of anomalies close to the subsequent epicenter often has been reported as an important but puzzling property of the radon precursor [Asimov et al., 1979; Teng, 1980b]. Because the number of observed anomalies shown in Figure 4 does not increase uniformly with distance, it is unlikely that the observed annulus effect is strongly dependent on the station density. The outer radius of the annulus increases slowly with the earthquake magnitude. The available data are not sufficient to tell whether the annular zone is continuous in azimuth. Although these results are strongly dependent on the available network of radon stations, they suggest a way of foretelling the expected earthquake magnitude.

The spatial distribution of radon anomalies of large amplitude appears to define a zone of precursor deformation that scales with the earthquake magnitude. Furthermore, short-term anomalies are more often observed far away from the subsequent rupture zone.

Interpretation

The interpretation of the data will be influenced by the experimental deficiencies that were pointed out in the last section. The interpretation can be useful, nonetheless, for comparing the radon data with other precursory data and theoretical models of earthquake precursors.

The increasing frequency of occurrence of radon anomalies with increasing magnitude can be explained in terms of a zone of precursory deformation that increases in size as magnitude grows. A large zone of precursory deformation is more likely to include several sensitive radon stations than a small zone. Since it is of relatively greater importance to study precursors to large earthquakes than to small ones, the frequency of occurrence constitutes a very useful property of the radon precursor. For instance, enhanced radon emission that could be induced by background seismicity in a seismic gap would be less likely to mask out anomalies related to a large event.

On the basis of a limited data set of radon anomalies as well as other precursors, Scholz et al. [1973] found a log-linear relation between precursor time and earthquake magnitude (see Figure 2). When comparing the almost continuous distribution of precursor times shown in Figure 2 with the Scholz et al. relation, one can see that the linear fit suggested by them represents approximately an average value for reported precursor times if the short-term anomalies associated with large earthquakes are neglected. The results of Figure 3 indicate that in most cases the precursor time interval is observed to be longer for stations located close to the future epicenter than for stations located far away. This pattern suggests a zone of precursor deformation that expands away from the future epicenter as the time of the earthquake approaches.

The amplitude data in Figure 4 are consistent with an almost circuar annulus around the future epicenter where the generation of radon anomalies is most favorable. The outer radius of the annulus increases slowly with earthquake magnitude, indicating that the spatial distribution of observed anomalies may be a measure of the expected earthquake magnitude. Often, the large amplitudes that are reported far away from the subsequent rupture zone have a short precursor time. This could be related to changes in the intensity of precursory deformation as the time of the earthquake approaches.

Thus a qualitative spatial and temporal pattern emerges from the available data. The precursor time interval scales with earthquake magnitude as well as with epicentral distance. The peak amplitude does not scale with magnitude but shows a consistent pattern with epicentral distance. The larger the earthquake magnitude, the larger the number of radon anomalies, and the farther away the largest amplitudes tend to occur. The radon anomalies therefore form a zone that expands slowly around the future epicenter and reflects more intense precursory deformation as the time of the earthquake approaches. The size of this zone scales with the magnitude of the impending earthquake.

Physical Basis

Most radon anomalies are observed outside of the future source region of the earthquake, and little is known about the detailed processes in the source region. Therefore a simple model of an inclusion embedded in an elastic matrix, such as the model of Rice and Rudnicki [1979], can be used to give a simplified description of the suggested physical basis. The inclusion that represents the source region is assumed to be defined by an elliptical rupture zone which could be determined, for instance, from the aftershock distribution. In the Rice and Rudnicki model, the stress-strain response of both the inclusion and its surroundings is time-dependent because both are presumed to be saturated by groundwater. Only the inclusion, however, can undergo dilatancy or inelastic deformation before the occurrence of the earthquake. The annulus where the radon anomalies are most often observed, as discussed in the previous section, is presumed to be mainly in the saturated surroundings with its inner boundary somewhat overlapping the outer edge of the inclusion.

The deformation of the surroundings, which is controlled by processes within the inclusion, can be roughly estimated by using the method of Dobrovolsky et al. [1979]. They assume a soft elastic, ellipsoidal inclusion in an elastic half space of 30% lower elastic modulus. The minor and major axes of the ellipsoid that are shown as dashed lines in Figure 5 also define an elliptical rupture zone. Calculated radii for strains, which represent the greatest distance where strain values of 10^{-6} and 10^{-8} can be detected, are shown in Figure 5 as a function of earthquake magnitude. Most of the radon anomalies in Figure 5 occurred between strain radii 10^{-6} and 10^{-8}, except for the radon anomalies related to earthquakes in the magnitude range between 7 and 8. This is, in part, caused by the formula that was used to convert magnitudes into rupture lengths, because it overestimates rupture lengths at large magnitudes [Dobrovolsky et al., 1979]. If the difference in elastic moduli between the matrix and the inclusion is smaller than 30%, the strains involved are even smaller. Strains of 10^{-6} to 10^{-8} are small enough to exclude mechanical crack growth induced by dilatancy as a possible mechanism for creating the observed anomalies.

A second possible mechanism, which consists of mechanical coupling between rock deformation and pore fluid diffusion, was suggested by Scholz et al. [1973] and Rice and Rudnicki [1979]. For such a mechanism to be effective, the loading rates or the associated strain rates have to be significantly faster than the time scales for the diffusion of local pore fluid. The values of strain that were obtained by the method of Dobrovolsky et al. [1979] at the sites of radon anomalies can be changed into values of minimum strain rate by taking the ratio between the strain values and the observed precursor time interval at that station. (This method of obtaining strain rates is similar to the one used by Bilham [1981] to obtain minimum strain rates from strainmeter data.) The strain rates that were found by using this method at

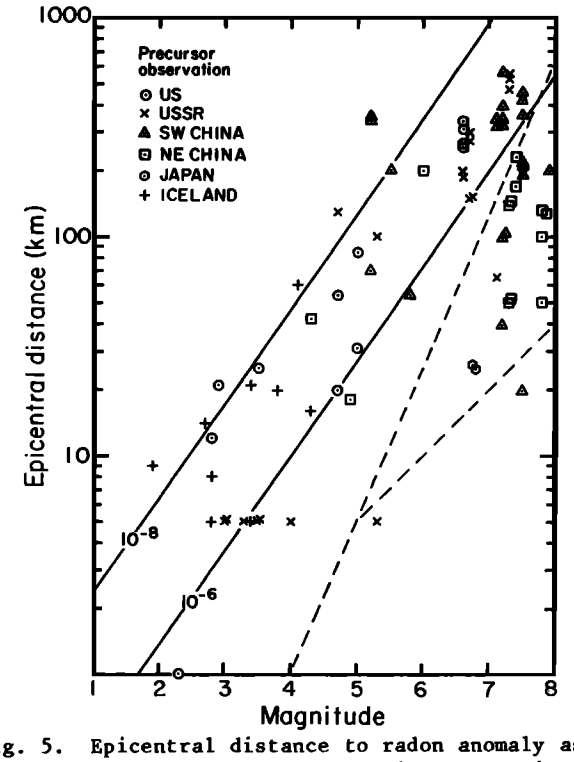

Fig. 5. Epicentral distance to radon anomaly as a function of earthquake magnitude. Lines 10^{-6} and 10^{-8} are theoretical predicted strain amplitudes as functions of earthquake magnitude and epicentral distance; dashed lines are the major and minor axes of the elliptical rupture zone [Dobrovolsky et al., 1979].

different sites of radon anomalies showed a total scatter from 10^{-6} day^{-1} to 10^{-10} day^{-1}. Most of the high strain rates that range from 10^{-6} day^{-1} to 10^{-7} day^{-1} result from overestimating the rupture lengths of large earthquakes as mentioned above. The strain rates that are smaller than 10^{-7} day^{-1} operate on time scales much longer than the time scales of the local pore fluid diffusion in shallow crustal rocks [Zoback and Byerlee, 1975]. Therefore it is rather unlikely that mechanical coupling between pore pressure and the rock matrix is responsible for the reported earthquake precursors.

Even though the changes in absolute strain levels presumed to occur during the precursory time interval appear to be small, very large changes in orientation of the local strain field could take place. Anderson and Grew [1977] propose stress corrosion in a water-saturated environment as a mechanism for tensile crack growth which could respond to such changes in the local strain field. Stress corrosion cracking has been observed in a fine-grained quartz rock (novaculite) and in granite under laboratory conditions at strain rates as low as 10^{-8} day^{-1} [Atkinson, 1980; Wilkins, 1980]. The purpose of these laboratory experiments was to determine the relationship between the crack velocity v of a tensile crack and the fracture mechanics parameter K_I, which is the stress intensity factor of the crack tip, under different environmental conditions. These K_I-v

relationships describe the complete time-dependent characteristics of tensile failure of a material [Atkinson, 1980]. If radon anomalies are indeed related to tensile failure controlled by stress corrosion, it is reasonable to expect that radon emission can somehow be described in terms of either a velocity of crack propagation or an average stress intensity factor.

In fracture mechanics the stress intensity factor for crack systems in uniform loading is defined as

$$K_I = m\,\sigma(\pi c)^{1/2} \qquad (1)$$

[Lawn and Wilshaw, 1975], where m is a dimensionless factor depending on geometry, σ is the remote applied stress, and c is the half length of the crack. Andrews [1977] studied radon emission in the laboratory as a function of rock particle size. He showed that the radon emission CR_n was proportional to the integrated boundary length b that intersects the surface of a rock particle:

$$CR_n = k \cdot b \qquad (2)$$

where k is a factor depending on the size distribution of rock particles and the mineral composition. By assuming that the 'integrated grain boundary length' is an equivalent quantity to the 'crack half length' above, it is possible to relate radon emission with the average stress intensity factor such that

$$CR_n \approx K_I^2 \qquad (3)$$

Thus the results of these two different laboratory experiments suggest that radon emission can be treated as a measure of the stress intensity factor for a local crack system in uniform tensional loading. The assumption that b is equivalent to c can be tested by monitoring acoustic emissions or hydrogen concentration in addition to radon content [Anderson and Grew, 1977; Wakita et al., 1980b].

The relationship in equation (3) between radon emission and stress intensity factor is in many respects supported by the worldwide data set of observed radon anomalies. In laboratory experiments the stress intensity factor varies by approximately a third of an order of magnitude; in the radon data set, the absolute amplitude of radon emission can change by approximately a half order of magnitude. The relative amplitudes that have been reported range from 5% to 500%, which corresponds to a change of at most a factor of 5 in absolute amplitude. The occurrence of anomalies with negative relative amplitude probably reflects a decreasing stress intensity factor. The inherent scatter in the radon data indicates that the generation of radon anomalies depends strongly on local conditions such as rock type, stress intensity factor, and degree of saturation.

A radon atom originates from the position of its parent radium isotope, which can occupy either some lattice site or an interstitial position in a crystal. Equation (2) assumes that the mechanism of radon release consists of recoil of the radon into crystal imperfections or grain boundaries, which provide paths for rapid diffusion into the surrounding groundwater [Andrews, 1977]. Other mechanisms such as direct recoil or lattice diffusion are considered to be less likely because of the low initial recoil energy of the radon atom, and a preferential distribution of radium isotopes in shallow surface layers of whole crystals has to be invoked [Tanner, 1980]. The model of stress corrosion implies that rocks that are rich in radioactive minerals have a mechanism of radon release similar to that of rocks containing small quantities of radioactive minerals. In the presence of water, however, radiation damage of radioactive minerals may significantly enhance the rate of radon release from those minerals [Tanner, 1980]. Since the radioactive damage usually consists of cylindrical or perhaps craterlike alpha tracks, the highly radioactive rocks may respond differently to applied stress or strain fields than rocks containing planar cracks. The contribution of alpha tracks to the total porosity can be approximately estimated as the track density times average track volume, or 10^{-7}% [Faure, 1977]. This result is negligible compared to the total porosity of, for example, granite (1/2-1%) and suggests that the behavior of cracks alone could account for the observed radon emission.

The time history or the shape of a radon anomaly is also affected by the local hydraulic properties. The peak amplitude depends on the distance of transport between the source rock and the radon station. In addition, the rise time and fall-off time of the anomaly are probably strongly influenced by hydrodynamic dispersion as well as the mechanism of radon release.

Discussion

The purpose of studying radon anomalies and other earthquake precursors is to develop the capability to foretell with reasonable accuracy the size, time, and place of a future earthquake in a geographic region of interest. This paper makes an attempt to evaluate the available worldwide radon data that have accumulated during the last 15 years and to assess whether the data can be applied for these purposes.

The data on precursor time demonstrate clearly that the log-linear relationship between the precursor time and the earthquake magnitude as interpreted by Scholz et al. [1973] does not apply, at least for radon anomalies. Thus forecasting the magnitude of a future event might require different and more complex methods than was previously thought. The radon data from regional networks suggest that the magnitude of the future event both determines the shape and the size of the region where radon anomalies are observed and controls the time history of the anomalous radon emission. A network of stations is therefore needed for telling the expected magnitude of the event instead of just a single station.

To forecast the time of the expected earthquake, the use of either precursor time from a precursor time versus magnitude plot, where the magnitude has been estimated by independent means, or the resumption of normal background values by several precursors just prior to the earthquake have been suggested. In the case of radon data, as was pointed out above, 'precursor time interval' does not scale in a simple way

with earthquake magnitude. Frequently, anomalous radon emission shows a different behavior immediately before the coming event. Radon stations that are located close to the future epicenter often show long-term anomalies that approach the background values just before the earthquake. At distant stations, where no anomaly or only a low-amplitude, long-term anomaly occurred, spikelike anomalies of several days duration signal the imminence of the future event. Therefore radon emission appears to have a large potential as an imminent precursor to foretell the time of the expected event.

From the spatial distribution of observed anomalies it can be seen that radon anomalies are rarely observed in the immediate vicinity of the subsequent rupture zone. Therefore it does not appear to be possible to evaluate from the radon data alone which fault out of several faults crosscutting a given region is the most likely one to rupture. The radon data, however, define a region within which the earthquake is most likely to occur, if a sufficient number of stations are available. Information about seismic gaps and other precursors such as strain, tilt, or V_p/V_s may then be used to identify the most likely fault zone.

This paper argues that the observed radon anomalies reflect small changes in the local stress intensity factor, which in turn controls the velocity of subcritical crack growth. This is supported indirectly by various laboratory experiments that determined crack growth [Anderson and Grew, 1977; Atkinson, 1979, 1980; Sobolev et al., 1978; Wilkins, 1980] and one laboratory experiment that determined radon emission as a function of the microstructure of the rock particles [Andrews, 1977]. No experiments have yet been performed that monitored both the stress intensity factor and the radon emission. Such experiments could prove useful for establishing a set of criteria to determine a priori whether a radon station is likely to show an anomaly.

Although the stress corrosion process is emphasized here, several other different mechanisms could explain the radon data. One possible mechanism would be large-scale regional strain events that cause both earthquakes and radon anomalies, as discussed by Shapiro et al. [1981] in southern California. Another mechanism that initially was proposed to explain linear and nonlinear variations in tidal admittance suggests that earthquake precursors may be related to accelerated tectonic stress rates [Beaumont, 1978].

Even though the set of worldwide radon data treated in this paper is rather extensive, the tentative interpretation and the suggested physical basis obviously will be subject to further development as more data accumulate. Detailed case studies of precursory data associated with both small and large earthquakes are needed as baseline data in future theoretical and experimental studies of radon anomalies and other earthquake precursors.

Conclusions

The main results of evaluating a worldwide set of radon data and comparing them with theoretical models are as follows:

1. The size of the region where radon anomalies are observed appears to scale with the earthquake magnitude and expand as the time of the earthquake approaches.
2. The radon data could be used to foretell the time of the expected earthquake by utilizing short-term anomalies and the return of long-term anomalies to normal background values.
3. Radon data by themselves only define a region, not a specific fault, where the earthquake is most likely to occur.
4. Radon data collected in different tectonic regions worldwide show similar and consistent properties.
5. Most of the observed radon anomalies occurred far away from the subsequent epicenter, and model calculations indicate that strain fields of at most 10^{-6} to 10^{-8} strain caused the anomalies. If these strains are divided by the appropriate precursor time, minimum strain rates from 10^{-7} day^{-1} to 10^{-10} day^{-1} are obtained.
6. The observed radon anomalies are thought to be caused by small changes in the local stress intensity factor, which in turn controls the velocity of slow crack growth in a wet environment.

Acknowledgments. The author wishes to thank Roger Bilham, Arthur Frankel, John G. Goddard, Lucile M. Jones, David Simpson, and Lynn R. Sykes for constructive discussions and reviews. This work was partly funded by the U.S. Geological Survey contracts 14-08-0001-17726 and 14-08-0001-19747. All the drawings were done by Patricia Catanzaro, and Mary Anne Avins skillfully typed the manuscript. Lamont-Doherty Geological Observatory contribution 3215.

References

Anderson, O. L., and P. C. Grew, Stress corrosion theory of crack propagation with applications to geophysics, Rev. Geophys. Space Phys., 15, 77-104, 1977.

Andrews, J. N., Radiogenic and inert gases in groundwaters, paper presented at 2nd International Symposium on Water-Rock Interaction, Strasbourg, France, Univ. Louis Pasteur, Centre Nat. Recherche Sci., Inst. Geol., Aug. 17-25, 1977.

Antsilevich, M. G., An attempt to forecast the moment of origin of recent tremors of the Tashkent earthquake through observations of the variation of radon (in Russian), Akad. Nauk. Uzb. SSR, 188-200, 1971.

Asimov, M. S., Zh. S. Yerzhanov, K. Ye. Kalmurzaev, M. K. Kurbanov, G. A. Mavlyanov, S. Kh. Negmatullaev, I. L. Nersesov, and V. I. Ulomov, The state of earthquake prediction research in the Soviet Republics of Central Asia (in Russian), International Symposium on Earthquake Prediction, Rep. III-12, 20 pp., UNESCO, Paris, 1979.

Atkinson, B. K., A fracture mechanics study of subcritical tensile cracking of quartz in wet environments, Pure Appl. Geophys., 117, 1011-1024, 1979.

Atkinson, B. K., Stress corrosion and the rate-dependent tensile failure of a fine-grained quartz rock, Tectonophysics, 65, 281-290, 1980.

Beaumont, C., Linear and nonlinear interactions between the earth tide and a tectonically stressed earth, Proceedings of the 9th GEOP Conference, Rep. 280, pp. 313-318, Dep. of Geod. Sci., Ohio State Univ., Columbus, 1978.

Bilham, R., Delays in the onset times of near-surface strain and tilt precursors to earthquakes, in Earthquake Prediction, Maurice Ewing Ser., vol. 4, edited by D. W. Simpson and P. G. Richards, pp. 411-421, AGU, Washington, D. C., 1981.

Craig, H., Y. Chung, R. Poreda, J. Lupton, and S. Damasceno, Fluid-phase earthquake precursor studies in southern California (abstract), Eos Trans. AGU, 61 (46), 1035, 1980.

Dobrovolsky, I. P., S. I. Zubkov, and V. I. Miachkin, Estimation of the size of earthquake preparation zones, Pure Appl. Geophys., 117, 1025-1044, 1979.

Faure, G., Principles of Isotope Geology, 464 pp., John Wiley, New York, 1977.

Hauksson, E., and J. Goddard, Radon earthquake precursor studies in Iceland, J. Geophys. Res., 86, 7037-7054, 1981.

Jiang, P., and Q. Deng, The development of precursory field and the tectonomechanical condition in the Haicheng-Tangshan earthquake series (in Chinese), Seismol. Geol., 2, 31-42, 1980.

King, C., Episodic radon changes in subsurface soil gas along active faults and possible relation to earthquakes, J. Geophys. Res., 85, 3065-3079, 1980.

Lawn, B. R., and T. R. Wilshaw, Fracture of Brittle Solids, Cambridge University Press, New York, 1975.

Liu, P. L., D. K. Wan, and T. M. Wan, Studies of forecasting earthquake in the light of the abnormal variations of Rn concentration in groundwater (in Chinese), Acta Geophys. Sin., 18, 279-283, 1975.

Mirzoev, K. M., A. S. Malamud, G. M. Rura, N. G. Salomov, O. V. Soboleva, and V. I. Starkov, The search for spatial and temporal regularities of changes in some parameters before large earthquakes, in The Search for Earthquake Precursors, pp. 241-250, Fan Publishers, Tashkent, USSR, 1976.

Raleigh, B., G. Bennett, H. Craig, T. Hanks, P. Molnar, A. Nur, J. Savage, C. Scholz, R. Turner, and F. Wu, Prediction of the Haicheng earthquake, Eos Trans. AGU, 58, 236-272, 1977.

Rice, J. R., and J. W. Rudnicki, Earthquake precursory effects due to pore fluid stabilization of a weakening fault, J. Geophys. Res., 84, 2177-2193, 1979.

Richter, C. F., Elementary Seismology, 768 pp., W. H. Freeman, San Francisco, Calif., 1958.

Rikitake, T., Earthquake precursors, Bull. Seismol. Soc. Am., 65, 1133-1162, 1975.

Rikitake, T., Classification of earthquake precursors, Tectonophysics, 54, 293-309, 1979.

Savage, J. C., W. H. Prescott, M. Lisowski, and N. E. King, Strain on the San Andreas fault near Palmdale, California: Rapid, aseismic change, Science, 211, 56-58, 1981.

Scholz, C. H., L. R. Sykes, and Y. P. Aggarwal, Earthquake prediction: A physical basis, Science, 181, 803-810, 1973.

Shapiro, M. H., J. D. Melvin, T. A. Tombrello, and J. H. Whitcomb, Automated radon monitoring at a hard-rock site in the southern California Transverse Ranges, J. Geophys. Res., 85, 3058-3064, 1980.

Shapiro, M. H., J. D. Melvin, T. A. Tombrello, M. H. Mendenhall, P. B. Larson, and J. H. Whitcomb, Relationship of the 1979 southern California radon anomaly to a possible regional strain event, J. Geophys. Res., 86, 1725-1730, 1981.

Sobolev, G., H. Spetzler, and B. Salov, Precursors to failure in rocks while undergoing anelastic deformations, J. Geophys. Res., 83, 1775-1784, 1978.

Sultankhodjaev, A. N., I. G. Chernov, and T. Zakirov, Hydrogeoseismic precursors to the Gazli earthquake (in Russian), Izv. Akad. Nauk. Uzb. SSR, 7, 51-53, 1976.

Szechwan Provincial Seismology Bureau (SPSB), The 1976 Songpan Earthquakes (in Chinese), 117 pp., Seismology Press, Peking, 1979.

Talwani, P., W. S. Moore, and J. Chiang, Radon anomalies and microearthquakes at Lake Jocassee, South Carolina, J. Geophys. Res., 85, 3079-3088, 1980.

Tang, C., Bases for the prediction of the Lungling earthquake and the temporal and spatial characteristics of precursors, Chin. Geophys., Engl. Trans., 1, 400-424, 1978.

Tanner, A. B., Radon migration in the ground: A supplementary review, Nat. Radiat. Environ., 1, 5-57, 1980.

Teng. T., Ground water radon content as an earthquake precursor, Geol. Surv. Open File Rep., U.S., 80-6, 357-360, 1980a.

Teng, T., Some recent studies on groundwater radon content as an earthquake precursor, J. Geophys. Res., 85, 3089, 1980b.

Ulomov, V. I., and B. Z. Mavashev, Forerunners of the Tashkent earthquakes (in Russian), Akad. Nauk. SSR, 188-200, 1971.

Wakita, H., Earthquake prediction and geochemical studies in China, Chin. Geophys., Engl. Transl., 1, 443-457, 1978.

Wakita, H., Y. Nakamura, M. Noguchi, and T. Asata, Radon anomaly-Possible precursor of the 1978 Izu-Oshima-Kinkai earthquake, Science, 207, 882, 1980a.

Wakita, H., Y. Nakamura, I. Kita, N. Fujii, and K. Notsu, Hydrogen release: New indicator of fault activity, Science, 210, 188-190, 1980b.

Wallace, R. E., and T. Teng, Prediction of the Songpan-Pingwu earthquakes of August 1976, Bull. Seismol. Soc. Am., 70, 1199-1223, 1980.

Wang, C. Y., Some aspects of the Tangshan (China) earthquake of 1976, Chin. Geophys., Engl. Transl., 1, 157-172, 1978.

Wilkins, B. J. S., Slow crack growth and delayed failure of granite, Int. J. Rock Mech. Min. Sci. Geomech. Abstr., 17, 365-369, 1980.

Zoback, M. D., and J. D. Byerlee, The effect of microcrack dilatancy on the permeability of Westerly granite, J. Geophys. Res., 80, 752-755, 1975.

(Received March 27, 1981;
revised July 1, 1981;
accepted July 31, 1981.)